

A Computational Study on the Moment Coefficient C_m of Formula One Exposed Dry and Wet-Condition Wheels

Mohamed Zakaria Soliman¹, Nabila S Elnahas¹, Mohamed A Abdelaziz^{1*} and Ahmed R El-Baz²

¹Automotive Department, Faculty of Engineering, Ain-Shams University, Egypt

²Mechanical Power Department, Faculty of Engineering, Ain-Shams University, Egypt

Abstract

A model of Formula One racing car rotating dry wheel in contact with the ground is studied using a computational approach as a validation case. This validation case focuses on the computed surface pressure around the wheel's center line. This computed result is compared to an experimental one obtained from the available literature work and it showed good agreement. Another case study is considered with replacing the dry wheel model with another wet-condition wheel model. The wet-condition wheel's work is mainly concentrated on the developed aerodynamic forces especially the wheel moment values. This moment is translated to an expression of resistive torque developed by the air stream on the wheel and computed in each case study. In addition, general schematic pictures of the flow behavior around the wet wheel are presented.

Keywords: Mechanical engineering; Automotive; Fluid mechanics; Aerodynamics; Formula wheel; Moment

Introduction

By the advent of the twenty-first century, road vehicle aerodynamics became less sensitive to the effect of body shape optimization which seems to have reached its limit. That was according to the automotive aerodynamicists' point of view that was based upon the effort spent on studying the effect of wheel rotation. Indeed, the term "body improvements" helped with the contribution of wheel aerodynamics to reveal significantly and become an interesting term especially in the case of open-wheel racing car, where the wheels are completely exposed to air and rotate against the flow direction which in turn affects the flow behavior and characteristics. Therefore, the wheels are the most influential components that affect the drag of Formula One racing car [1,2].

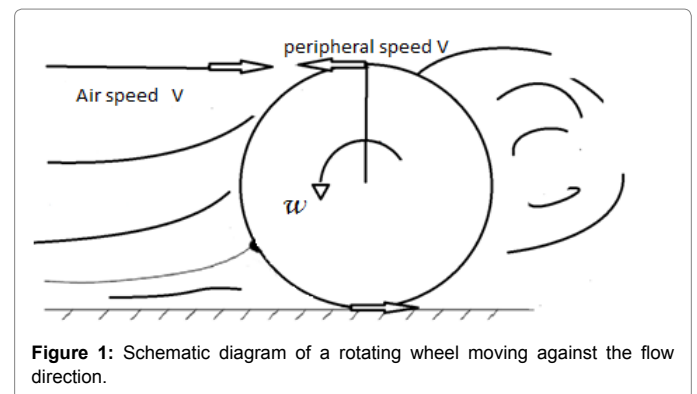
When considering the wing design, it is rational to consider the force needed to keep the wing moving through the air medium as a drag force.

On the other hand, in wheel design, the aerodynamic forces that represent the effort needed to keep the wheel rolling cannot be translated simply to the drag force. This is the problem which is associated with the study of the effect of wheel rotation. When comparing between both cases, rotating and stationary wheels, another additional parameter should be included in addition to drag and lift forces. This parameter is the resistive torque which is basically governed by the aerodynamic moment applied on the wheel. Figure 1 shows schematically the direction of flow stream and the direction of wheel rotation.

The resistive torque can be defined as the driving moment necessary to maintain the wheel rotation against the flow stream, while the car is travelling at steady speed. The effect of this resistive torque is expected to be high since the incoming air-flow doesn't simply attempt to force a stationary wheel to rotate in the clockwise direction, but it attempts to reverse the direction of a rotating wheel. The author also expects that the effect of the resistive torque would reveal significantly in the case of wet-condition wheel rather than the dry wheel. So, this work mainly focuses on computing the resistive torque in order to fairly judge the effect of wheel rotation on the car performance.

Various attempts have been made to measure the aerodynamic

forces acting upon a wheel in contact with the ground. These attempts have met with different levels of success and it was found that they depend on two basic methods (direct and indirect). The direct method is to measure the aerodynamic forces using a wind tunnel fitted with a balancing force device. The indirect method is to measure the surface pressure, using an electronic system inside the wheel, and integrate over the surface to derive the aerodynamic forces. Morelli [1] was the first to publish his work on the aerodynamic characteristics of an isolated wheel using the direct method. He tried to simulate the tire deformation by placing it into a rectangular recess in the ground-board with an unsealed 0.016D gap. It has been found that wheel rotation causes an increase in the drag nearby 10% over that produced in the case of stationary wheel.



***Corresponding author:** Soliman MZ, Automotive Department, Faculty of Engineering, Ain-Shams University, Egypt, Tel: +20 2 26831474; E-mail: m.zakaria_bb2@hotmail.com

Received January 07, 2017; **Accepted** February 20, 2017; **Published** February 28, 2017

Citation: Soliman MZ, Elnahas NS, Abdelaziz MA, El-Baz AR (2017) A Computational Study on the Moment Coefficient C_m of Formula One Exposed Dry and Wet-Condition Wheels. Fluid Mech Open Acc 4: 149. doi: [10.4172/2476-2296.1000149](https://doi.org/10.4172/2476-2296.1000149)

Copyright: © 2017 Soliman MZ, et al. This is an open-access article distributed under the terms of the Creative Commons Attribution License, which permits unrestricted use, distribution, and reproduction in any medium, provided the original author and source are credited.

Other researches were carried out by Stapleford and Carr [2]. Their experimental setup included a suspended wheel placed above a moving ground. An attempt to simulate the ground contact was performed using strips of paper mounted on the ground to seal the gap, but he couldn't simulate the wheel rotation and ground movement at the same time. Stapleford also recommend for the future work that a correct simulation for the flow problem requires perfect wheel rotation and ground contact, since the moving ground surface did not lead to significant improvements. The next to follow the same trend of interesting wheel studies was Cogotti [3]. His experimental setup could be adjustable in height in order to operate at various ground clearances. His results were similar to those of Stapleford and Carr [2].

On the other hand, Fackrell and Harvey [4,5] were the first to use the indirect method. They used the on-surface pressure integration to determine the net acting forces. This method was done by using a series of taps that were made through the wheel and were connected to an internal pressure transducer. Six wheels of varying profile and tread width, and of diameter 0.415 m, were tested to investigate the effect of rotation and the relationship between the net force and the aspect ratio. Fackrell's data confirmed that the effect of ground contact produces a significant lift as was concluded by Stapleford and Carr [2], and Cogotti [3]. He found out that there is pressure spike at the front of contact patch. So, he suggested developing a suction peak at the rear of contact patch. Hinson [6] evaluated the usability and suitability of the available-updated pressure measuring arrangement. Her data recorded the front spike which was investigated by Fackrell [5]. Hinson's work totally supported Fackrell's outcomes and came as a satisfactory evaluation to the updated measuring tool.

Another hardly-improved measuring system was developed Via Mears [7,8] by setting a pneumatic go-kart wheel in his experimental setup. This system led to a breakthrough observation allowing Mears to capture a suction peak at the rear of the contact patch. This was only proposed theoretically by Fackrell [5] in a non-approved manner. The next was Van Den Berg [9-13] whose work focused on investigating the aerodynamic interaction between the rotating wheel and the front inverted wing. Although his measuring arrangement was similar to that used by Fackrell, he didn't rely on the data collected by Mears which successfully captured the suction peak. He found that low pressure above the surface induced by the flow around the model can cause the belt to lift. Van Den Berg attempted to prevent that using suction on the underside of the belt and a suction peak was reported to be better.

Two highly-interesting papers, studying the effect of the contact area on the flow behavior and the wake structure were published. The first was by Purvis [9] who measured the base pressure located over several planes which lie normally to the upstream flow direction. By varying the degrees of the vertically applied force, data of various contact patch sizes versus vortices shape was collected. Purvis concluded mainly that as contact patch size (tire deformation) increases, the lobe vortices significantly increases. The second was by WÅaschle [10] who was the first to perfectly simulate a rotating wheel in contact with a moving ground using the direct method. His measurements were qualitatively in the same direction as the previously mentioned facts about the net lift and drag forces.

The first to use the CFD approach to simulate the wheel aerodynamics was Axon [11], in 1998. His primary dedication was to validate the usability of this technique. He modeled a simplified tire based on Fackrell's geometry. The results were compared to that obtained by Fackrell as a validation case. CFD approach could capture the front spike. Also, the wake size of the rotating wheel versus stationary was

observed. It was found that the vortices behind the rotating wheel were found to be much weaker, and closer to the wheel, than those behind the stationary wheel. Skea [12] applied a symmetry condition at the ground instead of a moving wall depending on Stapleford conclusion that moving ground surface did not lead to significant improvements. Consequently, the flow near the ground will slide smoothly rather than being forced to the direction of ground movement. The differences between these two approaches may not affect the results significantly; however, it is preferred to consider the moving wall condition since it is more realistic.

Dry Wheel Model

In spite of the high level of confidence in the Ansys simulation package used, a representative work should be done in addition to the main case study. This representative work is called verification case, which will also support the main case study by defining the most reliable conditions of testing. These conditions are the optimal mesh method and size, the flow volume size, and the best turbulence model.

In the validation model, a qualitative evaluation is based on the C_p values obtained computationally at the wheel's centerline. Figure 2 compares the obtained C_p values graphically to the experimental ones. In general, realizable k- ϵ model shows good agreement with the experimental data. However, lack in capturing the values of C_p is noticed in the spike at the front of contact patch and the drop in its back.

Model

In this work, a 50% scale model of formula one dry wheel is created according to the experimental model of Van Den Berg [13]. The model was developed using Ansys design modeler V 14.5 and Figure 3 shows the details of the dry wheel model used such as the tyre and its grooves dimensions. The boundary of the flow volume surrounding the tire is set according to the recommended dimension ratios in literatures [11,12]. The length in front of the tire is taken to be 5D and equal to the lengths of both sides and of the top [13]. The length behind the tire is set to be 15 D to be far enough to capture the large wakes and turbulence developed there as shown in Figure 4.

The usual demand in the meshing process is how to create a reliable model that gives accurate results, putting in mind the computational economic demands. In this work, the meshing process is limited due to lack of computational resources which restrict the max number of element around One million elements. In a better manner, for the urgent sake of economic model, the flow domain is divided into two parts in order to maintain a hybrid mesh with different grid sizes.

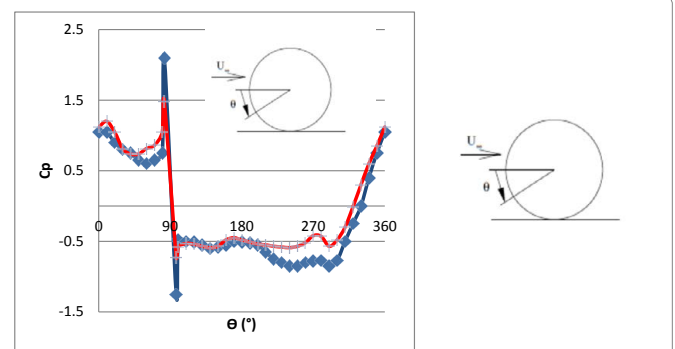


Figure 2: The comparison bet the computed results of surface pressure C_p vs. the angle θ (red) with the experimental one (blue).

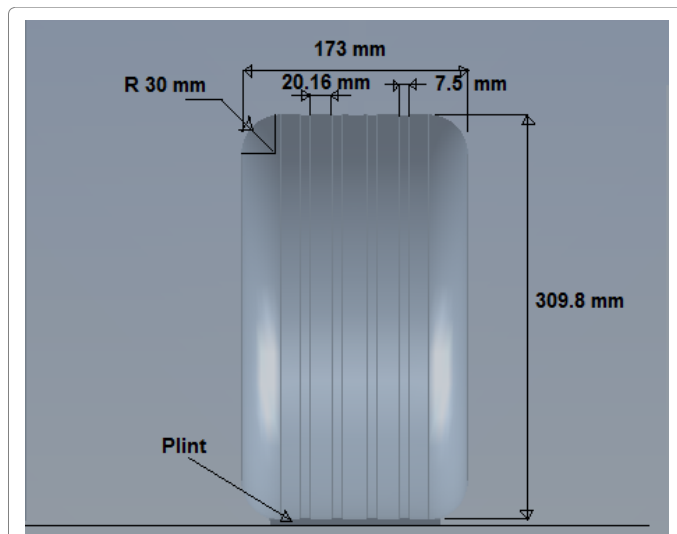


Figure 3: Geometry of the dry-condition wheel model used in the used by Van Den Berg.

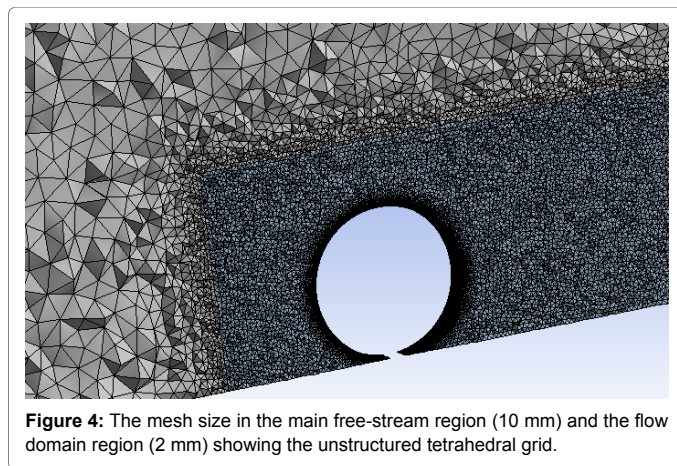


Figure 4: The mesh size in the main free-stream region (10 mm) and the flow domain region (2 mm) showing the unstructured tetrahedral grid.

The first is the main free-stream region which has slightly affected flow characteristics. The second region is the flow domain around the tire including the down-stream region which has strongly affected flow characteristics. This is depicted in Figure 4 which illustrates the different mesh size of both regions.

The meshing was generated using Ansys meshing module V14.5. It should be noted that, the meshing size has a significant impact on the accuracy of the solutions. Therefore, adjusting the mesh size over the flow domain region is an important factor in prediction results. A strategy is set to minimize the mesh size over the region surrounding the tire and keep it fixed over the free-stream region (2 mm). This strategy is performed on four steps of minimization starting with the coarse mesh size (100 mm), moving to the medium mesh (50 mm), and finally ending with the fine mesh sizes (10 mm, 5 mm). As will be shown later, both the fine mesh sizes (10 mm and 5 mm) produce approximately equal results. So, the 10 mm step is considered to be the grid independence size and all later work will be performed using this step size.

Governing equations and turbulence models

In this work, the considered equations are the conservation of

mass and momentum since there is no heat transfer or compressibility involved. Another additional transport equations are related to the turbulent flow is taken into account as well. the used Reynolds-averaging mass and momentum conservation equations for incompressible flow can be written as follows:

$$\frac{\partial}{\partial x_i}(\tilde{n}u_i) = 0 \quad (1)$$

$$\frac{\partial}{\partial t}(\rho u_i) + \frac{\partial}{\partial x_j}(\rho u_i u_j) = -\frac{\partial p}{\partial x_i} + \frac{\partial}{\partial x_j} \left[\mu \left(\frac{\partial u_i}{\partial x_j} + \frac{\partial u_j}{\partial x_i} - \frac{2}{3} \delta_{ij} \frac{\partial u_k}{\partial x_k} \right) \right] + \frac{\partial}{\partial x_j}(-\rho \overline{u_i u_j}) \quad (2)$$

Where the term of $-\overline{u_i u_j}$ is Reynolds stresses which is modeled in order to close Equation.

The used k-ε turbulence model is a semi-empirical two-equation model in which the solution of two separate transport equations allows the turbulent velocity and length scales to be independently determined. This model has robustness, economy, and reasonable accuracy for a wide range of turbulent flows in the aerodynamic simulations [13]. The turbulence kinetic energy, k, and its rate of dissipation, ε, and transport equations of the standard k-ε model are obtained respectively as follows:

$$\frac{\partial}{\partial t}(\rho k) + \frac{\partial}{\partial x_i}(\rho k u_i) = \frac{\partial}{\partial x_j} \left[\left(\frac{\mu_t}{\sigma_k} \right) \frac{\partial k}{\partial x_j} \right] + G_k - \rho \epsilon - Y_M + S_k \quad (3)$$

And,

$$\frac{\partial}{\partial t}(\rho \epsilon) + \frac{\partial}{\partial x_i}(\rho \epsilon u_i) = \frac{\partial}{\partial x_j} \left[\left(\frac{\mu_t}{\sigma_\epsilon} \right) \frac{\partial \epsilon}{\partial x_j} \right] + C_{1\epsilon} \frac{\epsilon}{k} (G_k) - C_{2\epsilon} \rho \frac{\epsilon^2}{k} + S_\epsilon \quad (4)$$

This turbulence model was generally used for all cases in this work. It should be noted that, using the one equation Spallart Allmaras (SA) model at the beginning of the solution, recovers the hard conversions. Also, the turbulent dissipation was set higher than normal to prevent excessive growth of the turbulence at the wake region in the first stages of the run. This in fact, also serves well in lowering the effect of hard conversions. Iterations are done to verify the applicability of non-equilibrium wall function and it is good approach. Therefore, in this work, near wall treatment is used to predict the flow behavior over the tire's surface and Y+ is adjusted to be within the range of 30-500.

All the studied cases have been solved using segregated RANS solver in implicit form and SIMPLEC scheme for the pressure - velocity coupling. In addition, the gradient of the grid was set to node based, which is more suitable for tetrahedron grid. Due to the abrupt change in flow variables near the contact region, the double precision option is set. All differential schemes are second order accurate, with the momentum and turbulence quantity equations being resolved with upwind discretizations.

Boundary conditions

The main boundary conditions were defined as velocity inlet to the inlet surface, pressure outlet to the outlet surface, wall to the tire and ground surfaces, and symmetry to the sides and top planes. Considering the inlet, choosing the velocity inlet makes it possible to define the velocity of the up-stream as 30 m/s. Also the turbulent intensity is set to be 10% as experimentally executed and turbulence viscosity ratio was assumed to be 10^{-7} as recommended for external flow. Considering the outlet, the backflow pressure was set to the atmospheric pressure datum. The ground was defined as a smooth moving wall with a translation velocity of 30 m/s and without slipping condition. In a same manner, the tire surface was defined as a smooth

wall without slipping condition but with a rotational speed 120 rad/s. The remaining boundaries such as the two side and the top surfaces of flow volume are defined as symmetry plane.

Wet Wheel Model

Starting from this section, the main case study will be the new design of formula one tire for the wet road condition. This design has other interesting features compared to the slick tire. These different features are mainly related to the tread pattern. Therefore, this study aims to eventually understand the effect of pattern design on the tire aerodynamics' coefficients.

The model of wet wheel is drawn to scale by using Ansys design modellerV14.5 also. The tire model's shape and dimensions were created according to the specifications of the Bridgestone Potenza F1 tire (20X7.5-13). Also, other interesting features related to the tread pattern are depicted in Figure 5. The flow domain will remain as adjusted in the validation work. But, another splitting has been developed around the wheel in order to create a rotating zone. This is a new technique for representing the region of the rotating flow near the tire wall. This was achieved using RRF (Rotating Reference Frame) method. The RRF method depends on including the dynamic effect of flow rotation mathematically while the mesh remains stationary.

As previously done in the validation case, all meshing techniques were developed over the flow domain. Also, a mesh size of 10 mm around the tire is created and the size of bounded elements to the tire was adjusted to maintain the Y^+ value from 30 to 300. Tetrahedron grid is created for all domains due to the high level of geometry complicity especially near the wheel surface as depicted in the Figure 6.

Along the same line of the previous work, the k-ε realizable turbulence model with non-linear wall treatment was selected. Also,

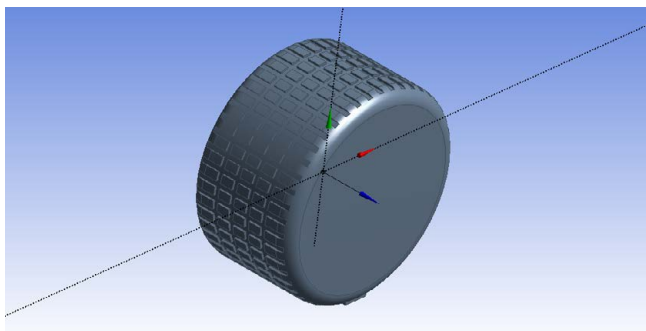


Figure 5: The Computational model of the wet-condition wheel used.

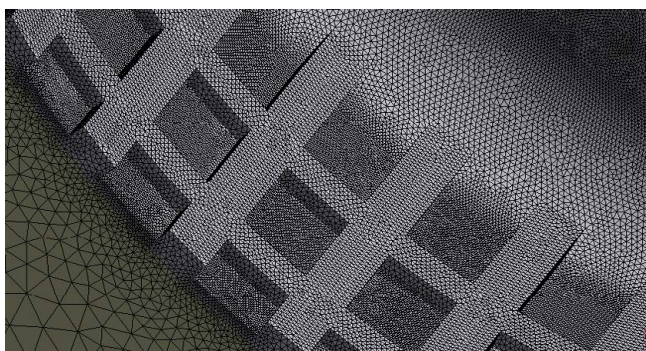


Figure 6: the tetrahedron grid near the wheel surface with the size of 2 mm.

all the same solver options and flow features were set as the validation case except for the steady flow. It has been found that, the unsteady flow option is far better in conversions than the steady one. That's due to the effect of existing tread pads which results in highly turbulent flow around tire surface. All boundary conditions were set to be identical to the last setup of validation work except for the tire motion. In addition, the new domain of circular zone around the tire is defined as RRF and has a rotational speed of 120 rad/s.

Results and Discussion

For all obtained results, it should be noted that the pressure coefficient C_p is calculated using the following equation:

$$C_p = \frac{2(p - p_\infty)}{\rho U_\infty^2} \quad (5)$$

Where P is the local pressure value, ρ is the air density computed under the atmospheric conditions, and U_∞ and p_∞ are the velocity and pressure of the upstream flow, respectively. Another dimensionless coefficient for the wheel C_m , defined by:

$$C_m = \frac{2T_r}{\rho R A_f U_\infty^2} \quad (6)$$

Where F_d is the total drag force applied on the wheel, F_l is the net lift force applied on the wheel, T_r is the resistive torque developed on the wheel, R is the wheel radius, ρ is the air density computed under the atmospheric conditions, and A_f is the frontal wheel area.

The wet wheel model has been first tested by varying the flow speed from 100 to 350 km/hr according to the formula one speed range. This evaluation was to ensure that the RRF can efficiently predict the C_m values and compare between the two cases (wet vs. dry wheel model). It has been found that the coefficient of C_m remain approximately constant under speed variation in both cases. This gives conceptual results from the aerodynamic point of view. This is shown in Figure 7, the moment coefficient is independent on the speed variation

The interesting part in these results is that the C_m has an average value of -0.085 and -0.014 in both wet and dry wheel model respectively. The negative sign indicates that the aerodynamic moment applied on the wheel is a resistive moment. This emphasizes that the incoming flow acts against the wheel rotation and resist its motion as was suggested earlier. Based on these results, the resistive torque reaches a value of 31 N.m at the max speed of 350 km/hr for wet wheel model and 5.7

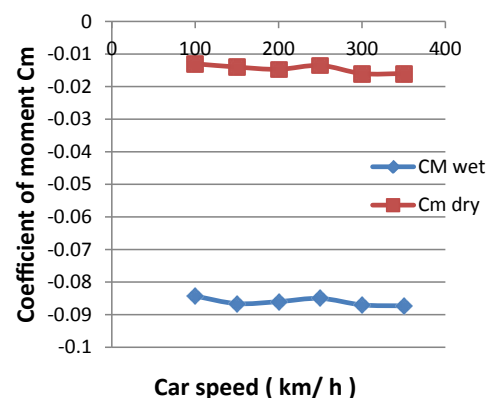


Figure 7: The relation bet the coefficient of moment C_m and the car speed in the cases of dry and wet wheel models.

N.m for the dry one. This is shown in Figure 8 which demonstrates the relation between the resistive torque and the car speed. Also, It should be noted that the resistive torque increases with the square of speed increasing. That is, when the speed doubles, the resistive torque will increase fourfold.

The previous results gathered with figures of pressure contours

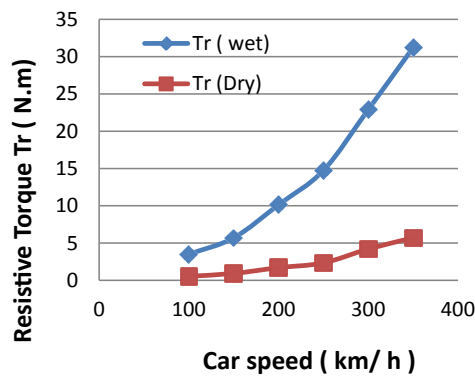


Figure 8: The relation bet the resistive torque and the car speed in the cases of dry and wet wheel models.

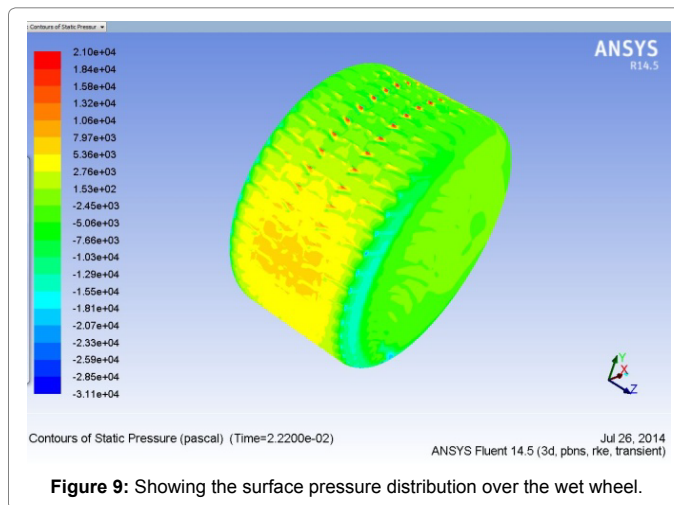


Figure 9: Showing the surface pressure distribution over the wet wheel.

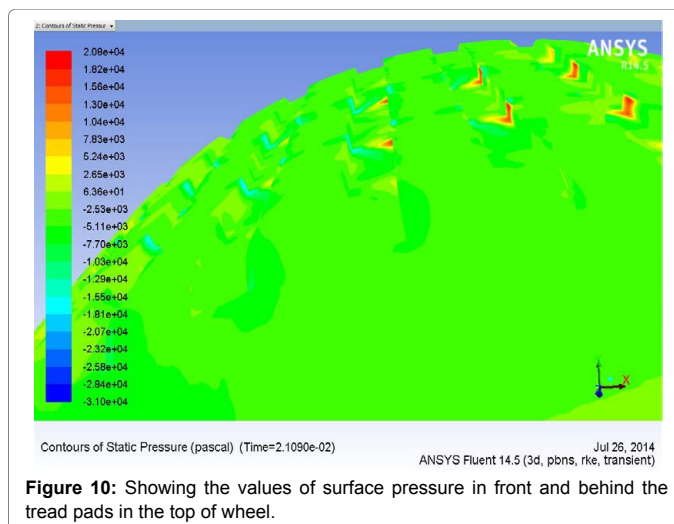


Figure 10: Showing the values of surface pressure in front and behind the tread pads in the top of wheel.

on the top of the wet wheel are presented. The interesting observation in Figure 9 is that the pressure values at the front of tread pads are greater than that at their back. This emphasized the phenomena of high leverage effect of the resistive torque on the top of the wheel. Figure 10 shows the surface pressure distribution over the whole wet wheel model. Also, some flow features such as the turbulent boundary layer near the wet wheel surface and the flow separation are depicted as shown in Figures 11 and 12 respectively.

Conclusion

Based on the obtained results from the computational analysis, many conclusions were extracted and summarized into three main points as follows:

1. The Ansys Multi-physics simulation package deals well with the analysis of flow around wet tires. In general, it shows good agreement to the experimental work in the verification case study as well as totally reasonable outcomes related to the wet wheel study.

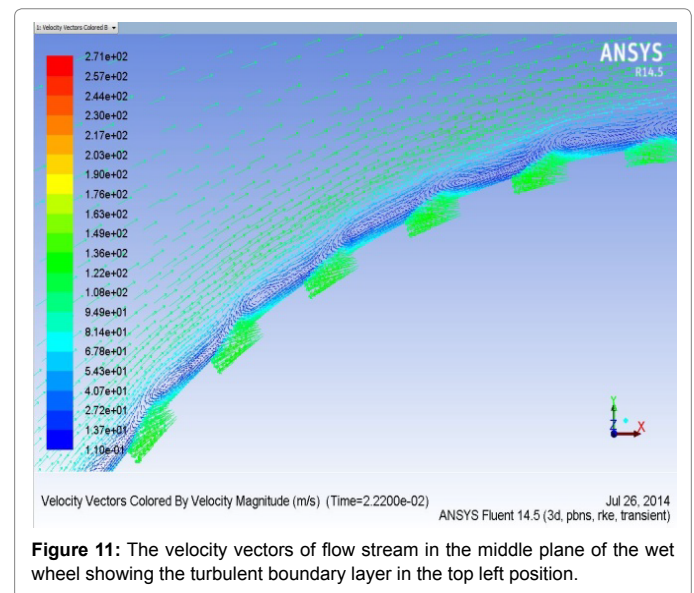


Figure 11: The velocity vectors of flow stream in the middle plane of the wet wheel showing the turbulent boundary layer in the top left position.

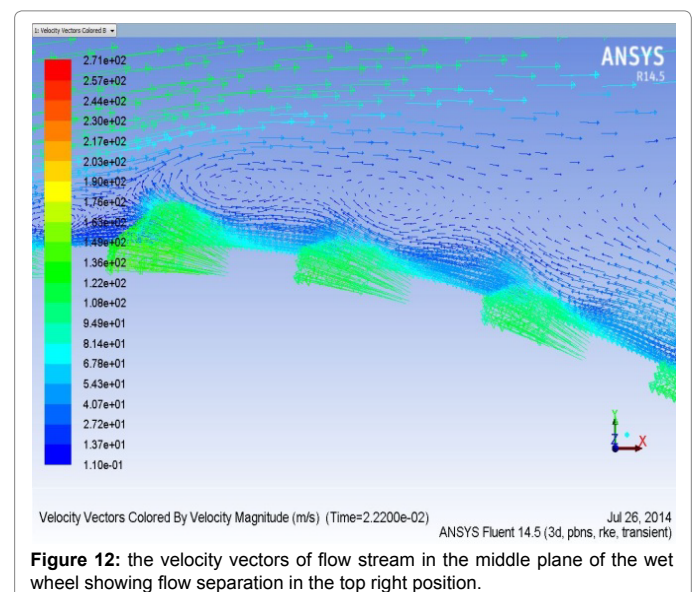


Figure 12: the velocity vectors of flow stream in the middle plane of the wet wheel showing flow separation in the top right position.

2. The realizable K- ϵ model with the non-linear wall treatment is a good approach in capturing the flow physics and features near the wheel surface such as the turbulent boundary and the flow separation. But there was a lack in predicting the spike and the drop in the C_p values in the validation case. In addition, the RRF technique shows a relatively good approach to simulate the dynamic effect of the wheel rotation.

3. The values of the resistive torque are high as was suggested by the author especially in the wet wheel model. Consequently, the resistive torque has a high leverage effect on the wheel aerodynamic performance and is a new parameter which has to be considered.

References

1. Morelli A (1969) Aerodynamics actions on an automobile wheel. In: *Procof 1st Symposium on Road Vehicle Aerodynamics*. Paper 5, City University, London.
2. Stapleford WR, Carr GW (1970) Aerodynamic characteristics of exposed rotating wheels Report 1970/2, Motor Industry Research Association, Nuneaton, UK.
3. Cogotti A (1983) Aerodynamic characteristics of car wheels. *Int J Vehicle Design, Technological Advances in Vehicle Design Series, SP3, Impact of Aerodynamics on Vehicle Design*, pp: 173-196.
4. Fackrell JE (1974) *The Aerodynamics of an Isolated Wheel Rotating in Contact with the Ground* PhD thesis, University of London.
5. Fackrell JE, Harvey JK (1974) The aerodynamics of an isolated road wheel in proc of AIAA 2nd Symposium on Aerodynamics, Competition Automobiles, Los Angeles, CA 16: 119-125.
6. Hinson M (1999) Measurement of the Lift Produced by an Isolated, Rotating Formula One Wheel Using a New Pressure Measurement System MSc thesis. Cranfield University.
7. Mears P, Dominy RG, Sims-Williams DB (2002) The flow about an isolated rotating wheel – Effects of yaw on lift, drag, flow structure. In: *Procof 4th MIRA International Vehicle Aerodynamics Conference*, Warwick, UK.
8. Mears P, Dominy RG (2004) Racing car wheel aerodynamics - Comparisons between experimental, CFD derived flow-field data. Technical Paper 2004-01-3555, Society of Automotive Engineers, Warrendale, PA.
9. Purvis R (2003) *The Wake Behind a Deformable Racing Tire*, MSc thesis, Cranfield University.
10. WÁaschle A, Cyr S, Kuthada T, Wiedemann J (2004) Flow around an isolated wheel- experimental, numerical comparison of two CFD codes. Technical Report SAE Technical Paper Series SAE.
11. Axon L, Garry K, Howell J (1998) An evaluation of CFD for modeling the flow around stationary, rotating wheels. Technical report, SAE Publication 980032.
12. Skea AF, Bullen PR, Qiao J (1998) The use of CFD to predict the air flow around a rotating wheel, *International Conference On Vehicle Aerodynamics*, UK.
13. Van MA, Berg D (2007) "Aerodynamic Interaction of an Inverted Wing with a Rotating Wheel" University of Southampton. *J Fluids Eng* 131: 101104.